Overview on Machine Vision Methods for Finding Defects in Transparent Objects

Johannes Meyer

Vision and Fusion Laboratory
Institute for Anthropomatics
Karlsruhe Institute of Technology (KIT), Germany
johannes.meyer@kit.edu

Technical Report IES-2015-XX

Abstract:
Machine vision methods are widely and successfully used for assuring the quality of any produced goods. Many of these methods require the test object's surface to be either nearly Lambertian or specular. Since transparent materials do not meet these requirements, suitable approaches for the inspection of transparent materials are needed. This paper provides an overview on existing methods for testing transparent objects for enclosed impurities, defects affecting the shape or anomalies of the index of refraction. Besides, possible topics for conducting further research are identified.

1 Introduction

Transparent materials play an important role in many fields of industries. They are often used in tasks or to create products that require high material quality and reliability, e.g., windshields for aircrafts and automobiles or high-precision optical elements like lenses used for guiding laser beams in medical surgery applications [Mey14]. Therefore, it is a common visual inspection task to check transparent objects for (enclosed) contaminants like absorbing particles (e.g., dust), scattering structures (e.g., air bubbles, surface scratches) or defects affecting the macroscopic 3D-geometry. For many applications, also the homogeneity of the material's refractive index is of utter importance. However, it cannot be evaluated by the naked human eye since it is not capable of observing phase effects. In general, the visual inspection of transparent objects is a fatiguing task for humans. The risk that the inspector oversees a material flaw increases notably after a small period of in-

spection time. This clarifies the importance of automated methods for the visual inspection of transparent objects.

There are many elaborated methods for inspecting opaque or specular objects. However, these methods are not applicable to transparent objects, for example, the laser lines employed by many active pattern projection systems cannot be observed on the test objects surface due to its transparency. Research has been performed to develop inspection methods suitable for transparent objects. This paper reviews the research results of the past years with respect to the automated testing of transparent objects for absorbing or scattering impurities, surface flaws, defects affecting the object's macroscopic 3D-geometry and for anomalies of the index of refraction. Since many of the reviewed methods follow an individual and complex approach they are described in dedicated sections.

2 Transmission setup

In common transmission setups for visual inspection, an undirected light source illuminates the test object from one side and a camera system observes the transmitted radiation on the test object's other side (see Fig. 2.1) [BLF15, ANW+09]. If the camera is focused on the test object, such setups are able to visualize absorbing contaminants. However, depending on the object's shape and index of refraction, some parts of the test object might not be inspected because the illuminating light rays can partly miss the camera [Hec13]. The setup cannot visualize scattering defects as—due to the undirected illumination—the light rays that miss the camera because of the scattering will not lead to a local intensity drop since other rays with another angle of incidence are likely to be scattered into the camera instead.

3 Dark field setup

In dark field setups the test object is usually illuminated in such a way, that in the case of a defect-free test object, no light reaches the camera (see Fig. 3.1). So, a defect-free test object results in a dark inspection image. Conversely, any scattering defect present in the transparent object will scatter the incident light into multiple directions—especially into the camera [BLF15, ANW+09, Hec13].

In general, dark field illumination is also capable of visualizing surface flaws like scratches. However, defects affecting the macroscopic 3D-geometry or inhomogeneities of the object's index of refraction cannot be visualized.

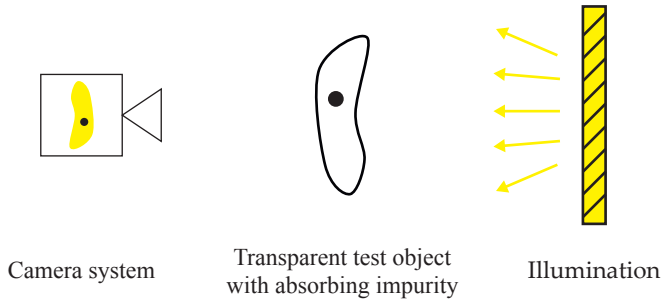

Figure 2.1: Conventional transmission inspection setup: An undirected light source illuminates the test object from one side. The transmitted light is observed by a camera system from the other side. Absorbing defects present in the test object appear as dark structures in the camera image.

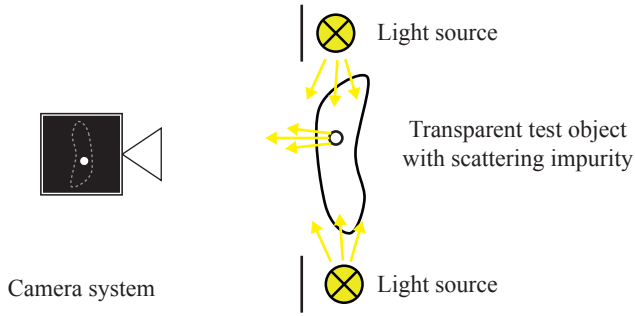

Figure 3.1: Conventional dark field inspection setup: One or more light sources, which are not in the camera's view, illuminate the test object. Any scattering impurity inside or on the test object will scatter some light into the camera and will result in bright structures in the observed image.

4 Retroreflection system

In order to overcome the limitations of the transmission setup (see Sect. 2) regarding test objects of complex geometry and with a high index of refraction, Hartrumpf et al. proposed an approach—the so-called Purity system [HH09, HVLS08, MLP+10]—that employs a retroreflective foil. Besides, their approach is able to simultaneously capture a dark field illuminated image by means of color multiplexing the different illumination sources.

Figure 4.1 shows a sketch of the respective optical setup. For obtaining the transmission image, a bright field illumination shines onto the test object out of the camera's direction via a beam splitter. The retroreflector—which is placed behind the test object—reflects any incident light ray back into its original direction. Since the Helmholtz reciprocity principle [Hec13] holds, the retroreflector compensates the refraction effect occuring at the interface between the transparentn object and the surrounding medium. This is why the Purity system is also capable of inspecting test objects having a complex geometry or a high index of refraction.

Besides the common dark field illumination described in Sect. 3, the approach uses an additional dark field illumination that shines on the test object with an angle of incidence that is close to Brewster's angle. This illumination visualizes small scattering contaminants located on the test object's surface. By employing individual colors (red, green, blue) for the different illumination components, a single acquired color camera image contains the information of all three illumination setups in separate channels.

Although it can capture absorbing or scattering impurities and surface flaws, the Purity system is not capable of visualizing defects affecting the test object's macroscopic 3D-geometry or its index of refraction. However, since the resulting inspection images require only simple image processing routines, the method's implementation is suitable for real-time applications.

5 Structured illumination system

In order to check complex-shaped transparent objects, e.g., headlamp lenses of automobiles, for absorbing or scattering impurities and for surface defects, Martínez et al. employ a robotic platform that moves a so-called 'binary active lighting system' around the test object [MOGG12]. Their illumination approach uses a monitor displaying a moving binary black and white stripe pattern (see Fig. 5.1). They require the test object to have no cavities and that the front and back surface are parallel to each other. Any scattering defect on or inside the test object will result in a deflection of rays. The deflection causes that some light of a displayed bright strips produces a bright spot in the camera image of one of the adjacent dark stripes (see Fig. 5.2). Conversely, an absorbing defect will result in a dark structure in the image of the corresponding bright stripe. By phase shifting the binary pattern and capturing multiple images, the test object is successively scanned.

Because of the robot platform, the setup can inspect even objects with a complex 3D-geometry. However, a sensor planning strategy has to be found for every type

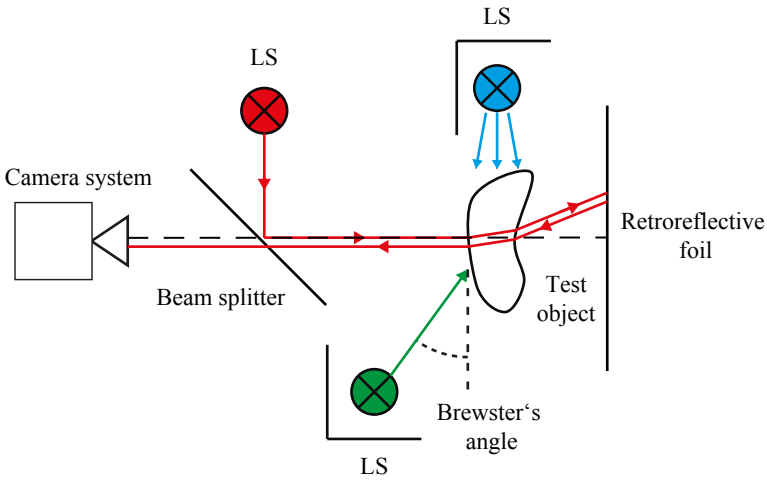

Figure 4.1: Setup of the Purity system: Via a beam splitter, the test object is illuminated from the direction of the camera's optical axis (red). A retroreflective foil placed behind the test object mitigates refraction effects occurring at the interfaces between the test object and the surrounding medium. A dark field illumination (blue) visualizes scattering defects. A third light source (green) illuminates the test object under Brewster's angle in order to visualize surface contaminants, e.g., dust particles.

of test object. The proposed approach is not capable of visualizing defects affecting the macroscopic 3D-geometry of the object or its index of refraction.

6 Transmissive optical shearing interferometer

Seo et al. employ digital holographic microscopy in order to detect surface scratches on transparent cover glasses with a magnitude of less than 10^{-6} m [SKKK14, SKK14]. Their proposed setup is based on a transmission-type optical shearing interferometer as shown in Fig. 6.1.

An expanded coherent laser beam illuminates the test object. The transmitted light is collected by a microscope lens and directed onto a shearing element, i.e., a high-quality glass-plate with a thickness smaller than the laser's coherence length. The reflections from the front and back surface create hologram patterns on the sensor by interfering with each other.

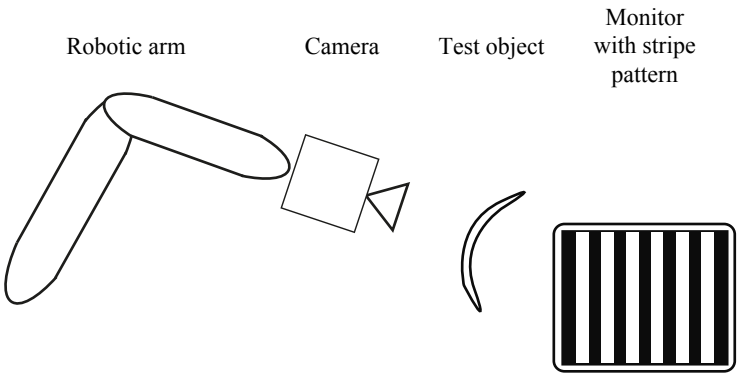

Figure 5.1: Structured illumination setup: A monitor realizes the 'binary active lighting system' and illuminates the test object. A camera observes the transmitted light. In order to inspect the whole test object, a robotic arm moves the camera to precomputed positions.

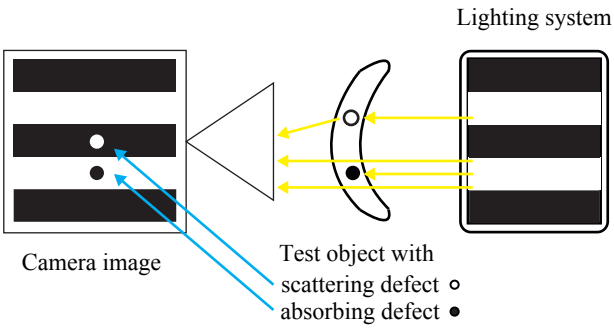

Figure 5.2: Defect visualization by means of the 'binary active lighting system': Absorbing defects are imaged to dark structures if illuminated by a bright stripe. Scattering defects are visualized by causing bright regions in the images of adjacent black stripes.

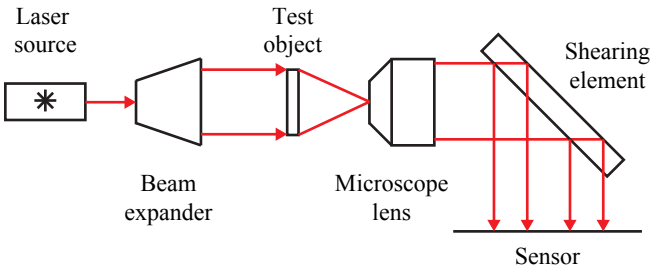

Figure 6.1: Transmissive optical shearing interferometer: An expanded coherent laser beam illuminates the test object. The transmitted light is collected by a microscope lens that magnifies the test object. A shearing element tilted by 90° directs the light onto a sensor, where the reflections from the shearing element's front and back surface interfere with each other. The resulting hologram is captured by the sensor.

By acquiring two holograms—one with the inserted test object and one without it—the thickness of the investigated object can be reconstructed and can reveal surface scratches.

Although the author has only applied the presented approach to find defects affecting the test object's surface structure, it should also be appropriate to detect inhomogeneities of the index of refraction. However, the method cannot visualize absorbing or scattering impurities and defects affecting the macroscopic 3D-geometry.

7 Phase shifting interferometer

Chatterjee used a polarization phase shifting interferometer in order to test high-quality optical glass slabs for inhomogeneities of the local distribution of the index of refraction [Cha15]. An expanded laser beam is split into a reference arm and a probe arm. The test object is immersed into a liquid that matches the object's index of refraction. After the probe beam traversed the test object, it passes a quarter-wave plate and a rotatable linear polarizer together with the reference beam. In concert, the two beams create an interference pattern on a rotating diffuser screen that is used to reduce speckle. The screen is observed by a camera. Figure 7.1 shows the principle optical inspection setup.

By employing polarizing beam splitters and the quarter-wave plate, an adjustable phase-shift can be induced by rotating the linear polarizer. Capturing and process-

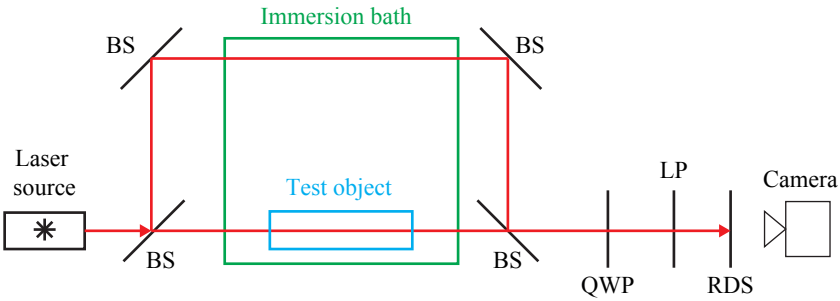

Figure 7.1: Phase shifting interferometer: A coherent laser beam is split into a reference arm (upper path) and a probe arm (lower path) by a polarizing beam splitter (BS). The probe arm passes the test object that is immersed in a liquid matching the test object's index of refraction. Another beam splitter recombines the two arms. A quarter-wave plate (QWP) and a rotatable linear polarizer induce an adjustable phase shift to the transmitted beam. A camera observes the interference pattern created by the two beams on a rotating diffuser screen.

ing images for different rotation angles of the linear polarizer allows to unwrap the phase information of the optical path difference conveyed in the interference patterns. The unwrapped phase can be used to detect inhomogeneities of the index of refraction with an accuracy of 10^{-6}.

8 Conclusion and future work

This contribution discussed some of the recent works regarding the automated visual inspection of transparent objects. Table 8.1 lists the covered methods and summarizes their suitability for industrial inspection applications.

Each of the presented approaches is capable of visualizing one or more of the considered defect types but none of them is sensitive to them all. Therefore, a possible topic for future research could be to find an inspection method that is able to capture all mentioned defect types.

Besides, industrial inspection tasks often pose challenging timing conditions that cannot be met by some of the discussed approaches. Hence, improving the image acquisition and processing speed of automated inspection methods for transparent objects represents another open research question.

	Absorbing impurities	Scattering impurities	Shape flaws	Macr.3D-geometry	Index of refraction
Transmission	+	-	-	-	-
Dark field	-	+	+	-	-
Retroreflection	+	+	+	-	-
Structured illumination	+	+	+	-	-
Shearing interferometer	-	-	+	-	-
Phase shifting interferometer	-	-	-	-	+

Table 8.1: Summary of the different approaches for defect visualization in transparent objects. +: the type of defect is visualized; -: the type of defect is not visualized.

Bibliography

[ANW+09] Gil Abramovich, Christopher Nafis, Yana Williams, Kevin Harding, and Eric Tkaczyk. Three-dimensional embedded defect detection and localization in a semi-transparent medium. In *Proc. SPIE*, volume 7432, page 74321C, 2009.

[BLF15] Jürgen. Beyerer, Fernando Puente León, and Christian Frese. *Machine Vision: Automated Visual Inspection: Theory, Practice and Applications*. Springer Berlin Heidelberg, 2015.

[Cha15] Sanjib Chatterjee. Determination of refractive index in-homogeneity of transparent, isotropic optical materials. In *Advances in Optical Science and Engineering*, pages 61–66. Springer, 2015.

[Hec13] Eugene Hecht. *Optics*. Pearson, San Francisco, 4th edition, 2013.

[HH09] Matthias Hartrumpf and Rüdiger Heintz. Device and method for the classification of transparent components in a material flow. Patent WO 2009/049594 A1, 2009.

[HVLS08] Matthias Hartrumpf, Kai-Uwe Vieth, Thomas Längle, and Günter Struck. Neues Verfahren zur Sichtprüfung transparenter Materialien. In *Sensorgestützte Sortierung*, pages 57–58, Aachen, March 2008.

Gesellschaft für Bergbau, Metallurgie, Rohstoff- und Umwelttechnik.

[Mey14] Johannes Meyer. Visual inspection of transparent objects – physical basics, existing methods and novel ideas. Technical Report IES-2014-04, Karlsruhe Institute of Technology, 2014.

[MLP+10] Wolfgang Melchert, Thomas Längle, Philipp Pätzold, Robin Gruna, and Michael Palmer. Automatische Sichtprüfung strukturierter transparenter Materialien. In *Forum Bildverarbeitung, F. Puente León und M. Heizmann, Hrsg., Regensburg, Germany*, pages 143–153, 2010.

[MOGG12] S Satorres Martínez, J Gómez Ortega, J Gámez García, and A Sánchez García. A machine vision system for defect characterization on transparent parts with non-plane surfaces. *Machine Vision and Applications*, 23(1):1–13, 2012.

[SKK14] Kwang-Beom Seo, Byung-Mok Kim, and Eun-Soo Kim. Digital holographic microscopy based on a modified lateral shearing interferometer for three-dimensional visual inspection of nanoscale defects on transparent objects. *Nanoscale research letters*, 9(1):1–14, 2014.

[SKKK14] Kwang-Beom Seo, Byung-Mok Kim, Jung-Sik Koo, and Eun-Soo Kim. A novel three-dimensional visual inspection scheme for defect detection of transparent materials based on the digital holographic microscopy. In *International Multidisciplinary Microscopy Congress*, pages 37–44. Springer, 2014.